ORIGINAL RESEARCH

Fibrosis of the Neonatal Mouse Heart After Cryoinjury Is Accompanied by Wnt Signaling Activation and Epicardial-to-Mesenchymal Transition

Makiko Mizutani, PhD; Joseph C. Wu, MD, PhD; Roeland Nusse, PhD

***Background*—**The adult mammalian heart responds to cardiac injury by formation of persistent fibrotic scar that eventually leads to heart failure. In contrast, the neonatal mammalian heart reacts to injury by the development of transient fibrotic tissue that is eventually replaced by regenerated cardiomyocytes. How fibrosis occurs in the neonatal mammalian heart remains unknown. To start elucidating the molecular underpinnings of neonatal cardiac fibrosis, we investigated Wnt signaling in the neonatal heart after cryoinjury.

***Methods and Results*—**Using expression of the Wnt target gene Axin2 as an indicator of Wnt/β-catenin signaling activation, we discovered that epicardial cells in the ventricles are responsive to Wnt in the uninjured neonatal heart. Lineage-tracing studies of these Wnt-responsive epicardial cells showed that they undergo epithelial-to-mesenchymal transition and infiltrate into the subepicardial space and exhibit fibroblast phenotypes after injury. In addition, we showed that—similar to adult ischemic injury—neonatal cryoinjury results in activation of Wnt signaling in cardiac fibroblasts near injured areas. Furthermore, through in situ hybridization of all 19 Wnt ligands in injured neonatal hearts, we observed upregulation of Wnt ligands (Wnt2b, Wnt5a, and Wnt9a) that had not been implicated in the adult cardiac injury response.

***Conclusions*—**These results demonstrate that cryoinjury in neonatal heart leads to the formation of fibrotic tissue that involves Wnt-responsive epicardial cells undergoing epithelial-to-mesenchymal transition to give rise to fibroblasts and activation of Wnt signaling in resident cardiac fibroblasts. **(*J Am Heart Assoc*. 2016;5:e002457 doi: 10.1161/JAHA.115.002457)**

Key Words: fibrosis • neonatal heart injury • Wnt signaling

A major feature of the adult cardiac repair response to ischemic injury is formation of fibrotic scar tissue. Following ischemic injury, the influx of cardiac fibroblasts to replace lost cardiomyocytes is critical for the structural integrity of the heart; however, the subsequent extracellular matrix deposition by cardiac fibroblasts and formation of persistent scar tissue ultimately leads to heart failure. Development of fibrosis after ischemic injury is a complex process that involves the resident cardiac fibroblasts as well as infiltrating fibroblasts of diverse origin. In particular, both epicardial[1] and endothelial[2] cells undergo epithelial-to-mesenchymal transition (EMT) to give rise to cardiac fibroblasts in response to injury. Much of how these diverse cell populations are regulated in the process of fibrosis formation remains to be elucidated.

Similar to the adult heart, the mammalian neonatal heart initially responds to cardiac injury by the formation of fibrotic tissue[3,4]; however, fibrosis in the neonatal heart is subsequently cleared and replaced by regenerated cardiomyocytes at 3 weeks after apical resection.[3] Dynamics of fibrotic tissue regression after cryoinjury seem to be more variable, with reports of complete scar regression within 3 weeks[5] and the presence of residual scar tissue up to 3 months after injury.[6] Although recent studies have started to identify factors that allow neonatal cardiomyocytes to proliferate in response to injury,[7,8] it remains unknown how fibrotic tissue develops in the neonatal heart. A better understanding of fibrosis in the neonatal heart may lead to the development of new strategies to treat permanent scarring in the adult heart.

A molecular signaling pathway that may play an important role in regulating the fibrotic response in the neonatal heart is Wnt signaling, a pathway already implicated in the adult

From the Department of Developmental Biology (M.M., R.N.), Stanford Cardiovascular Institute (J.C.W.), and Division of Cardiology, Department of Medicine (J.C.W.), Stanford University School of Medicine, Stanford, CA; Howard Hughes Medical Institute, Stanford University, Stanford, CA (R.N.).

Correspondence to: Roeland Nusse, PhD, Department of Developmental Biology, Stanford University, Lorry I. Lokey Stem Cell Research Building, 265 Campus Drive, Rm G2143B, Stanford, CA 94305. E-mail: rnusse@stanford.edu

Received October 27, 2015; accepted February 1, 2016.

cardiac injury response.[9] In the adult heart following myocardial infarction, various cell types, including epicardial cells, cardiac fibroblasts, and endothelial cells, become responsive to Wnt.[2,10] Wnt/β-catenin signaling activation in epicardial cells is critical for their proliferation and generation of cardiac fibroblasts by EMT.[10] Effects of Wnt signaling activation in the modulation of the overall fibrotic response are less clear, for example, blocking Wnt signaling by expression of peptides homologous to Wnt ligands (Wnt3a and Wnt5a)[11] or secreted frizzled-related proteins reduces infarct size.[12,13] Unexpectedly, expression of a constitutively active form of β-catenin by adenovirus-mediated transduction also reduces infarct size.[14] These findings illustrate the versatile and complex roles that Wnt signaling plays in the adult cardiac injury response.

Although the role of Wnt signaling has been studied in the adult heart injury response, it is unknown whether Wnt signaling is induced in the neonatal heart. In this study, we showed that epicardial cells are Wnt responsive in the uninjured heart and that these epicardial cells give rise to cardiac fibroblasts and myofibroblasts and contribute to scar tissue formation. In addition, we observed that neonatal cryoinjury results in activation of Wnt signaling, especially in the cardiac fibroblasts near the injury site. Furthermore, we conducted an in situ hybridization screen of all 19 Wnt ligands and identified specific Wnt ligands in injured neonatal hearts that are different from Wnt ligands previously reported to be upregulated in the adult cardiac injury response.

Methods

Animals

Axin2-lacZ,[15] Axin2-CreERT2,[16] and mTmG[17] mouse strains were backcrossed to FVB for at least 8 generations. All animal protocols were approved by the animal use and care committee of the Stanford University School of Medicine.

Neonatal Cryoinfarction

Neonatal cryoinfarction was performed, as described previously.[5] Briefly, neonatal mice on postnatal day 1 (P1) or P2 were anesthetized by hypothermia, the heart was exposed through an incision in the fourth intercostal space, and the apex of the heart was frozen for 10 seconds with a 1-mm diameter wire that had been cooled in liquid nitrogen. Following injury, the ribs were adapted with 6-0 Prolene sutures (Ethicon), and the skin was glued back together with a surgical glue (Butler Schein). Neonates were warmed up and returned to their mothers. Buprenorphine at a dose of 0.0015 mg/kg was given subcutaneously for analgesia at the time of surgery and later as needed. There were 3 or 4 mice in each experimental group.

Lineage Tracing Studies

Tamoxifen (Sigma-Aldrich) was dissolved in a corn oil/ethanol mixture (90%:10% vol/vol) and filtered through a 0.2-μm membrane filter. Neonates were injected with tamoxifen on P0 with 0.2 mg IP at 48 hours prior to injury or on P10 with 4 mg IP/25 g body weight at 9 days after injury.

Histology and Immunostaining

Heart samples were collected, washed briefly in PBS, incubated in 100 mmol/L potassium chloride for 5 minutes, rinsed in PBS, and then fixed in 4% paraformaldehyde at 4°C overnight. Following fixation, samples were washed in PBS, dehydrated through an ethanol series, cleared in orange terpene, and embedded in paraffin. Paraffin-embedded samples were sectioned at 5-μm thickness using a microtome and mounted on Superfrost microscope slides (Fisher Scientific). For trichrome staining, slides were stained using a Masson's trichrome staining kit (Pacific Southwest Lab Equipment). For immunostaining, paraffin sections were treated with Tris/EDTA (pH 9) for antigen retrieval. The following antibodies were used: chicken anti–green fluorescent protein (anti-GFP; 1:1000; Abcam), rabbit antivimentin (1:800; Abcam), mouse anti–cardiac troponin C (1:50; ThermoScientific), rabbit anti–fibroblast-specific protein 1 (1:100; Abcam), mouse anti–Wilms tumor 1(1:50; Dako), mouse anti–α-smooth muscle actin (anti–α-SMA; 1:800; Sigma-Aldrich) and rat anti-Ki67 (1:400; eBiosciences). Because of high background fluorescence in the GFP channel, Cy3- and Cy5-conjugated secondary antibodies were used. The samples were mounted with ProLong Gold Antifade mountant with DAPI (Invitrogen).

X-gal Staining

Heart samples were collected, washed briefly in PBS, and then fixed in PBS with 0.2% glutaraldehyde and 5 mmol/L EGTA for 1 hour at room temperature. Following fixation, samples were washed in detergent rinse (PBS with 2 mmol/L $MgCl_2$, 0.01% sodium deoxycholate, 0.02% NP-40) and then stained in a staining solution (PBS with 2 mmol/L $MgCl_2$, 0.01% sodium deoxycholate, 0.02% NP-40, 5 mmol/L potassium ferrocyanide, 5 mmol/L potassium ferricyanide, and 1 mg/mL X-gal) overnight at room temperature in the dark. After staining, samples were washed in detergent rinse, postfixed with 4% paraformaldehyde overnight at 4°C, and then dehydrated as described above.

RNA In Situ Hybridization

All in situ hybridization experiments were done using RNAScope (ACD Bio).[18] Both sham and cryoinjury samples were collected

at 9 days after surgery performed on P1 FVB wild-type neonatal mice. Samples were fixed in 10% neutral buffered formalin for 24 hours at room temperature. Following fixation, samples were rinsed with PBS, dehydrated, and embedded in paraffin. Paraffin-embedded samples were sectioned at 5-μm thickness and processed according to the manufacturer's instructions. The following probes were used for the Wnt ligand screen: Wnt1 (NM_021279.4, 1204-2325), Wnt2 (NM_023653.5, 857-2086), Wnt2b (NM_009520.3, 1307-2441), Wnt3 (NM_009521.2, 134-1577), Wnt3a (NM_009522.2, 683-1615), Wnt4 (NM_009523.2, 2147-3150), Wnt5a (NM_009524.3, 200-1431), Wnt5b (NM_001271757.1, 319-1807), Wnt6 (NM_009526.3, 780-2026), Wnt7a (NM_ 009527.3, 1811-3013), Wnt7b (NM_009528.3, 1597-2839), Wnt8a (NM_009290.2, 180-1458), Wnt8b (NM_011720.3, 2279-3217), Wnt9a (NM_139298.2, 1546-2945), Wnt9b (NM_011719.4, 727-1616), Wnt10a (NM_009518.2, 479-1948), Wnt10b (NM_011718.2, 989-2133), Wnt11 (NM_009519.2, 818-1643), and Wnt16 (NM_053116.4, 453-1635).

Microscopy and Imaging

Whole-mount images were taken with a Leica M80 microscope. All bright-field images and fluorescent immunostaining images except for images showing costaining against GFP and another marker were obtained using the Zeiss Axio Imager Z2. Fluorescent immunostaining against GFP and other markers was imaged using a Leica SP8 confocal microscope.

Quantitative Reverse Transcription Polymerase Chain Reaction Analysis

Heart samples were collected; sectioned into injured, border, and remote portions; and flash frozen in liquid nitrogen. Total RNA was isolated using the RNeasy fibrous tissue mini kit (Qiagen), following the manufacturer's instructions. cDNA samples were synthesized along with the control samples with no reverse transcription. Quantitative reverse transcription polymerase chain reaction was performed using the following Taqman probes: Snail1 (Mm00441533_g1, FAM) and GAPDH (Mm99999915_g1, VIC). Relative gene expression levels were calculated using the ΔΔCt method.

Statistical Analysis

For quantification of GFP-labeled cells, each treatment group had at least 3 independent samples obtained from different groups of mice such that there were no repeated measurements in the same individual at different time points. For each sample, multiple paraffin sections were made, and 4 to 5 fields of image per area of interest (area of injury, area bordering injury, and area located remotely from injury) were obtained to manually count labeled cells using ImageJ software (National Institutes of Health). The total number of cells per field was obtained by counting DAPI counterstain using the Cell Counter plugin for ImageJ. For each sample, the average percentage of labeled cells of interest from the total number of cells was calculated based on the values obtained from 4 to 5 fields of image. Two-way ANOVA analysis with ad hoc pairwise comparison using Dunnett's multiple comparison test was performed to compare values between the earliest time point (2 day) and later time points (7 and 21 days). All statistical analysis was performed using GraphPad Prism 6 software (GraphPad Software) and SAS (SAS Institute). The statistical values are shown as mean±SEM. P values <0.05 were considered statistically significant.

Results

Neonatal Epicardium and Atrial Cells are Wnt Responsive Without Injury

We examined neonatal hearts for Wnt signaling activity using Axin2-lacZ mice.[15] Axin2 is a Wnt target gene that reflects activation of Wnt/β-catenin signaling.[19] Whole-mount X-gal staining of neonatal (P1) hearts revealed the presence of Wnt-responsive cells in the atria, epicardium, and subepicardial space (Figure 1A through 1C). In addition, cardiac valves were also Wnt responsive, as reported previously, in the adult heart (Figure 1D).[2] Whole-mount X-gal staining of wild-type neonatal hearts showed no endogenous β-galactosidase activity (not shown).

To characterize the Axin2-positive cells and to track their fates, we used a lineage-tracing mouse, Axin2-CreERT2.[16] Axin2-CreERT2 mice express a tamoxifen-inducible Cre-recombinase from the Axin2 locus. When crossed with the reporter strain Rosa26-mTmG (mTmG),[17] a subset of Axin2-positive cells was labeled with membrane-bound GFP on tamoxifen administration. To determine the identity of Wnt-responsive cells in the neonatal heart, we administered tamoxifen in Axin2-CreERT2;mTmG mice at P0 and harvested the hearts 48 hours later for immunostaining analysis (Figure 1E through 1K). As expected, GFP-labeled cells in Axin2-CreERT2;mTmG mice recapitulated the Axin2-lacZ reporter expression pattern. In the ventricle, the majority of the labeled cells were epicardial cells coexpressing vimentin and Wilms tumor 1 and showing a flattened morphology on the surface of the myocardium (Figure 1E and 1F, arrowheads, and 1G, arrow). There were rare cardiomyocytes expressing cardiac troponin T, a cardiomyocyte marker in the subepicardial space (Figure 1G, arrowhead). In the atria, Axin2-positive cells coexpressed cardiac troponin T (Figure 1H). We also observed rare Axin2-positive interstitial cardiac fibroblasts and endocardial cells that coexpressed

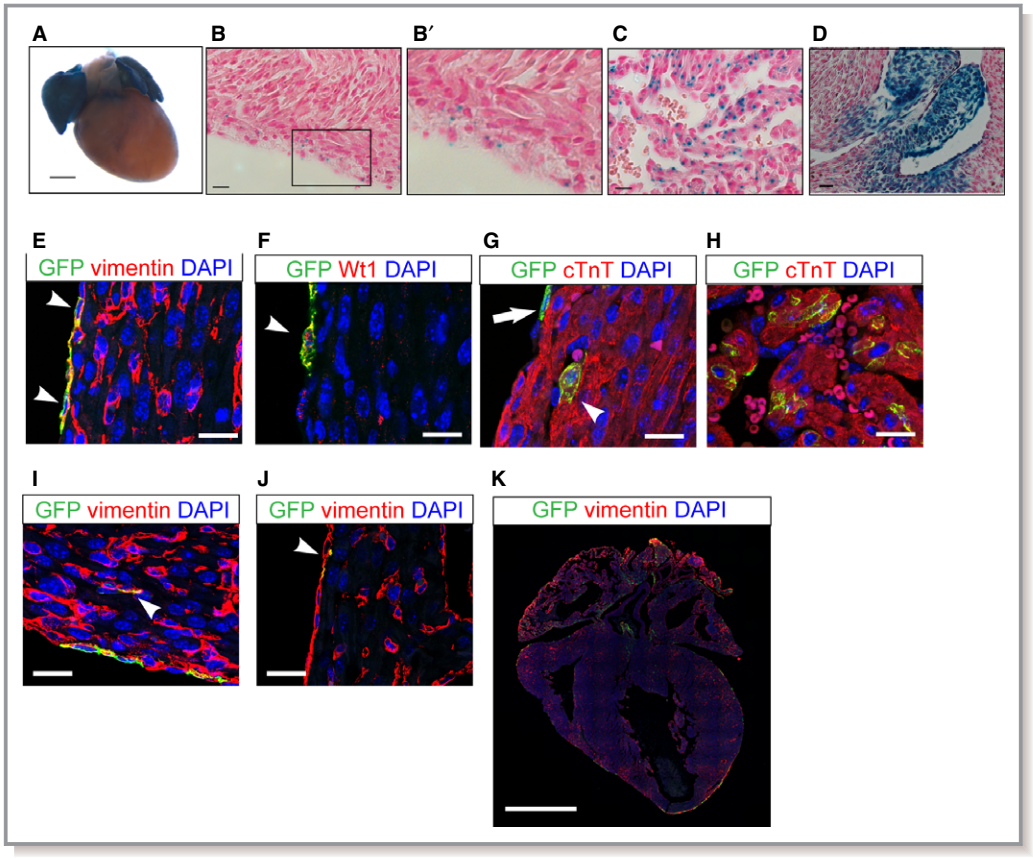

Figure 1. The neonatal heart atrial cardiomyocytes and epicardial cells are Wnt responsive. Neonatal heart of Axin2-lacZ mice at P1. A, Whole-mount X-gal staining of the neonatal heart. Scale bar=0.5 mm. B, X-gal staining of the epicardial and subepicardial space. B', Inlet enlarged from (B). C, X-gal staining of atrial cells. D, P1 neonatal heart of Axin2-lacZ mice showing Wnt-responsive cells of valves. B through D, Scale bar=10 μm. E through K, Immunofluorescent staining to characterize Axin2-positive cells using Axin2-CreERT2;mTmG neonatal heart labeled at P0 and traced for 2 days. E, Immunostaining against vimentin (red) and GFP (green) in the epicardium. Arrowheads indicate double-positive cells. F, Immunostaining against Wilms tumor 1 (Wt1) and GFP. Arrowhead indicates a double-positive cell. G, Immunostaining against cTnT and GFP in subepicardial cardiomyocytes. The arrow indicates a GFP-positive epicardial cell not positive for cTnT. The arrowhead indicates a double-positive cell. H, Immunostaining against cTnT and GFP in atria. I, Immunostaining against vimentin and GFP in the cardiac interstitium. Arrowhead indicates double-positive interstitial cells. J, Immunostaining against vimentin and GFP in the endocardium. Arrowhead indicates double-positive cells. E through J, Scale bar=20 μm. K, Immunostaining against vimentin and GFP in a lower magnification stitching image. Scale bar=1 mm. cTnT indicates cardiac troponin T; GFP, green fluorescent protein; P1, postnatal day 1.

vimentin (<0.03%) (Figure 1I and 1J). Our results revealed the presence of Wnt-responsive cells in the uninjured neonatal heart.

Wnt-Responsive Epicardial Cells Undergo EMT to Give Rise to Cardiac Fibroblasts After Cryoinjury

The epicardium provides multipotent cardiac progenitors during both embryonic development and adult injury response.[20–23] During adult myocardial infarction, the epicardium becomes Wnt responsive and gives rise to cardiac fibroblasts.[10] Because little is known about the role of the epicardium in the neonatal cardiac injury response, we asked whether the Wnt-responsive epicardial cells we observed in the neonatal heart contributed to the cardiac injury response. To address this question, we performed cryoinjury, as described previously.[5,6]

To track the fate of Wnt-responsive epicardial cells following cryoinjury, we administered tamoxifen to Axin2-CreERT2;mTmG mice at P0, performed cryoinjury 48 hours later at P2, and then examined the hearts after various time points (Figures 2A and 3). At 2 days after injury, the majority of GFP-labeled cells (GFP^+ cells) in the ventricles were located in the epicardium in both sham hearts (90.1±2.7%) and

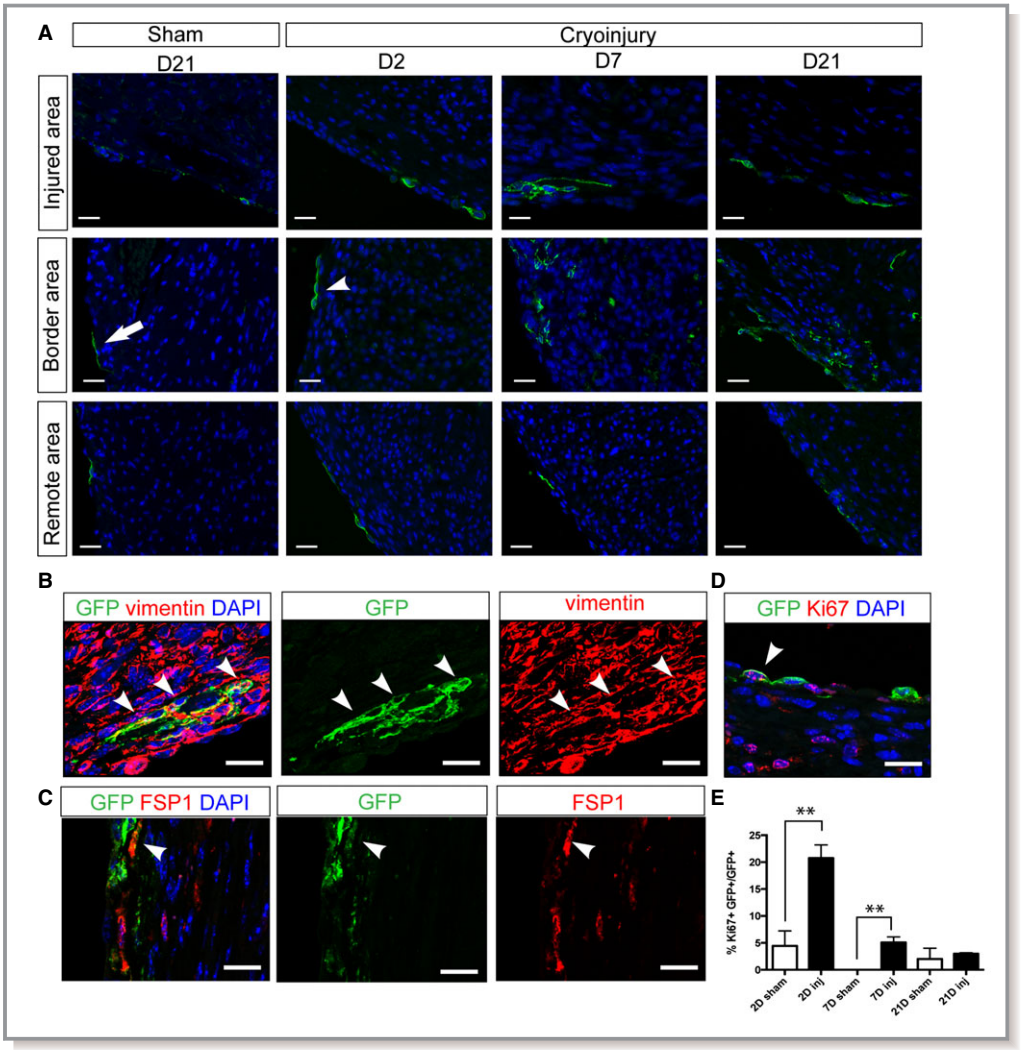

Figure 2. Wnt-responsive epicardial cells infiltrate myocardium and exhibit a fibroblast marker. Axin2-CreERT2;mTmG neonates were labeled at P0, underwent cryoinjury or sham surgery, and were sacrificed at various time points. A, Representative pictures of injured hearts showing injured areas, border areas, and remote areas at 2, 7, and 21 days. Corresponding areas from sham-treated hearts at 21 days after surgery are also shown. B, Immunostaining against GFP (green) and vimentin (red) in the injured heart at 7 days after injury. Arrowheads indicate double-positive cells. C, Immunostaining against GFP (green) and FSP1 (red) in Axin2-CreERT2;mTmG neonates that received TM before injury on P0 and were traced for 7 days. Arrowhead indicates double-positive cell. D, Immunostaining against GFP (green) and Ki67 (red) in the injured heart at 2 days after injury. The arrowhead indicates a double-positive cell. A through D, Scale bar=20 μm. E, Quantification of the percentage of GFP- and Ki67-positive cells in the border area in injured hearts and the equivalent area in sham-operated hearts at 2, 7, and 21 days after surgery. Each group had at least 3 independent samples. Multiple fields (4–5) from an individual sample were imaged. Values are represented as mean±SEM. $^{**}P<0.01$. F through H, Quantification of the percentage of GFP and vimentin double-positive cells in (F) the injured area, (G) the border area, and (H) the remote area of injured hearts and the equivalent areas in sham-operated hearts at 2, 7, and 21 days after surgery. Each group had 3 independent samples (n=3). Multiple fields (4–5) from an individual sample were imaged. Values are represented as mean±SEM. $^{*}P<0.05$. I, Quantitative reverse transcription polymerase chain reaction analysis of the Snail1 expression in the border area of the injured or sham-operated hearts at 1, 3, 7, and 9 days after surgery. Each group had 3 independent samples (n=3). The Snail1 expression level of day 1 sham-operated hearts is set to be the control. The fold change was calculated using the ΔΔCt method. J, Schematic of the experimental time line. K, Diagram indicating the injured area, the border area, and the remote area. Red represents viable myocardium, and blue represents fibrotic tissue. B indicates border area; D indicates day; FSP1, fibroblast-specific protein 1; GFP, green fluorescent protein; I, injured area; Inj, injured; P, postnatal day; R, remote area; TM, tamoxifen.

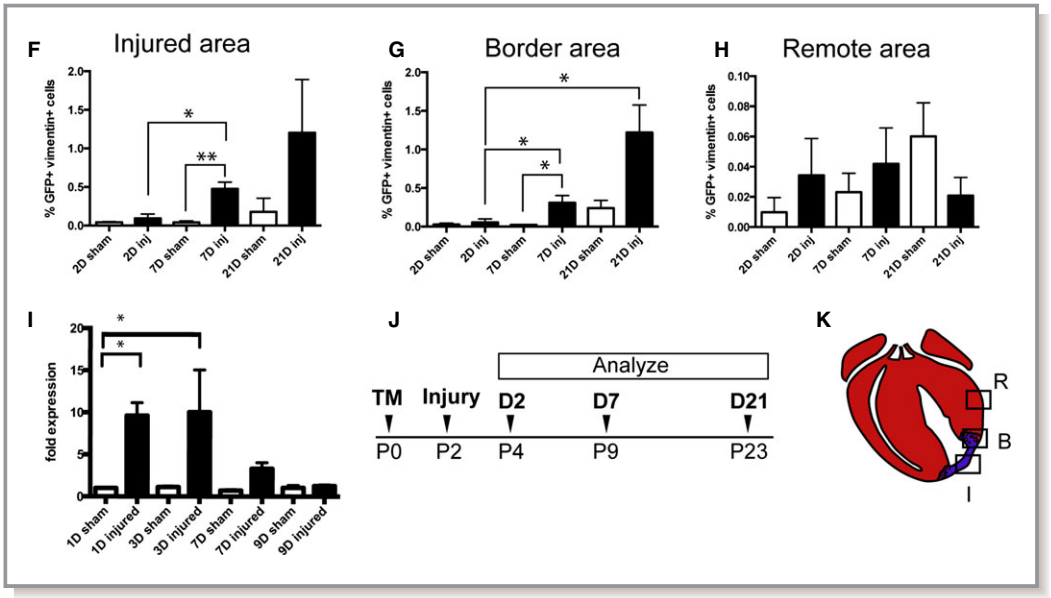

Figure 2. continued.

cryoinjured hearts (92.0±2.7%). Even though the distributions of the GFP$^+$ cells were similar for both sham and injured hearts, it is interesting to note that the GFP$^+$ epicardial cells within and near the injured area exhibited a rounded morphology (Figure 2A, arrowhead), whereas the GFP$^+$ epicardial cells in sham-operated hearts were thin and flat (Figure 2A, arrow).

By 7 days after injury, compared with the sham-operated group, we observed a significant increase in the number of GFP$^+$ cardiac fibroblasts that coexpressed vimentin (GFP$^+$/vimentin$^+$) within the injured area as well as in the border area where surviving myocardium mingled with fibrotic tissue (Figure 2A, 2B, 2F, and 2G). These GFP$^+$ cells also coexpressed another cardiac fibroblast marker, fibroblast-specific protein 1 (Figure 2C). Within the injured area, GFP$^+$/vimentin$^+$ cells in the subepicardial space increased 5.2-fold between 2 and 7 days after injury (P<0.05) (Figure 2F). In the border area, GFP$^+$ cardiac fibroblasts in the myocardium accounted for 0.05±0.04% (n=4) of the total cell number at 2 days after injury. The percentage of GFP$^+$ cardiac fibroblasts within the myocardium increased 6-fold by 7 days after injury and 24-fold by 21 days after injury (P<0.05) (Figure 2G). We observed that fibrosis containing these GFP$^+$ cardiac fibroblasts persisted for at least 8 weeks after injury (Figure 4A and 4C). In contrast, there was no significant difference in the percentage of GFP$^+$ cardiac fibroblasts in remote areas at different time points after injury (Figure 2H). In sham-operated hearts, there was a trend of increased percentages of GFP$^+$ cardiac fibroblasts in the comparable areas, but the difference was not significant at different time periods (Figure 2D and 2H). This result suggests that Wnt-responsive epicardial cells also may contribute to cardiac fibroblasts in normal postnatal development at a slower rate.

One of the key features of cardiac injury response in the adult heart is the activation of cardiac fibroblasts to become myofibroblasts. To determine whether Wnt-responsive epicardial cells also give rise to myofibroblasts, we examined α-SMA expression. At 2 days after injury, we observed no GFP$^+$ cells that costained with α-SMA (Figure 5). At 7 days after injury, there were rare GFP$^+$/α-SMA$^+$ cells in the border area, accounting for 0.04±0.01% of the total cell number and 8.4±1.4% of the GFP$^+$ cell number (Figure 5B and 5C). At 21 days after injury, there were virtually no GFP$^+$/α-SMA$^+$ cells (Figure 5B and 5C). In sham-operated hearts, we never observed GFP$^+$ cells that costained with α-SMA at any of the time points examined (Figure 5).

To assess whether these Wnt-responsive epicardial cells proliferate in response to injury, we examined Ki67 expression in the border area where we observed a significant increase in the number of GFP$^+$ cells. At 2 days after injury, we readily observed GFP$^+$ epicardial cells that costained with Ki67 (Figure 2D). In fact, there was a significantly greater percentage of GFP$^+$ cells costained with Ki67 in the injured group than in the control group (P<0.01) (Figure 2E). Also at 7 days after injury, there were significantly more Ki67$^+$/GFP$^+$ cells in the injured group compared with the control group (P<0.01) (Figure 2E). There was no significant difference between the injured and control groups by 21 days after injury. Furthermore, to assess whether there was evidence of EMT, we performed quantitative reverse transcription polymerase chain reaction analysis to examine the expression of an EMT marker, Snail1, in the injured and control groups at

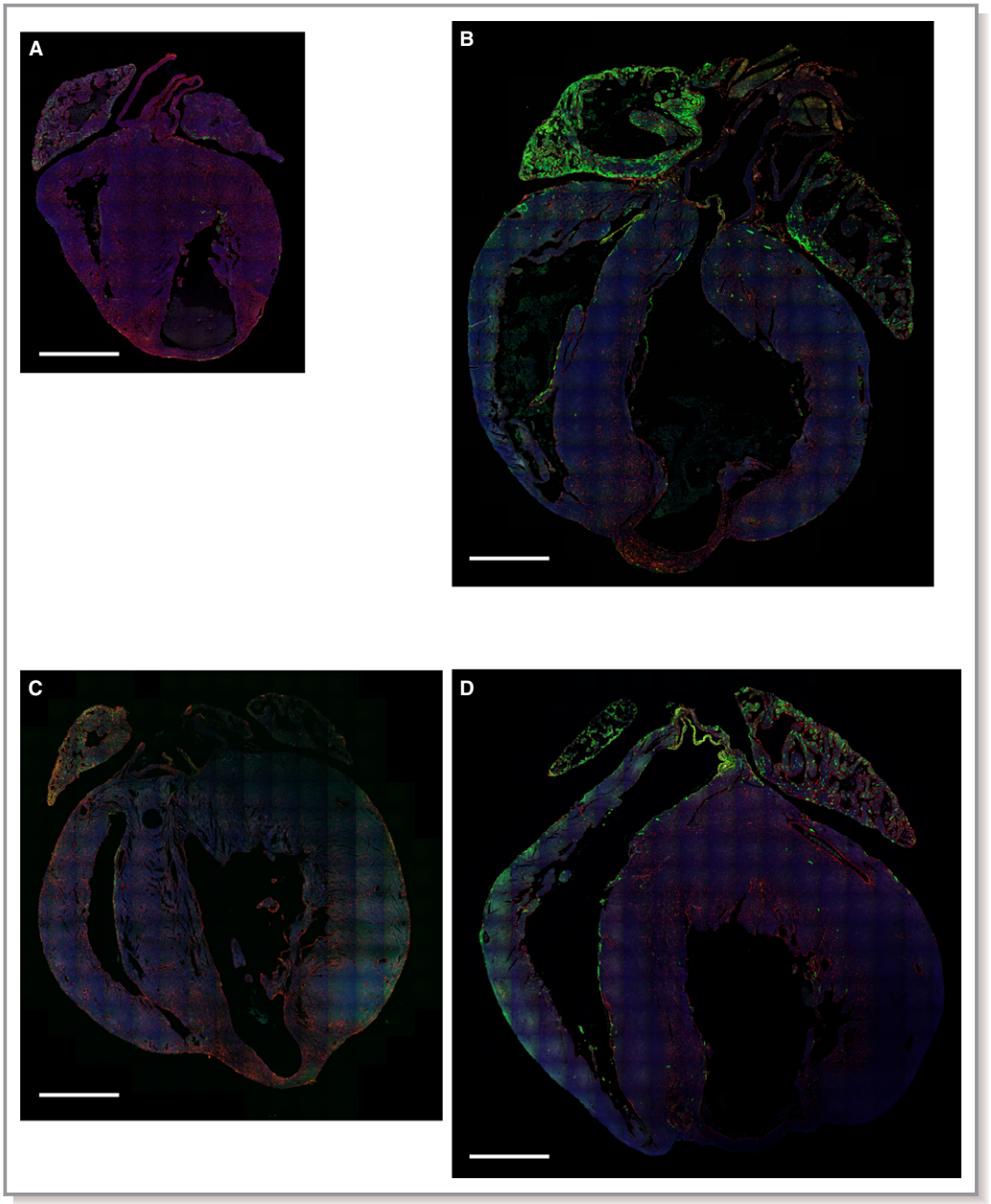

Figure 3. Low-magnification images of Axin2-CreERT2;mTmG hearts after injury. Axin2-CreERT2;mTmG mice were given tamoxifen on P0, underwent cryoinjury, and then were traced for 2 days (A) or 21 days (B). Axin2-CreERT2;mTmG mice were given tamoxifen at 9 days after cryoinjury and then traced for 2 days (C) or 21 days (D). Scale bar=1 mm.

various time points. We found that the expression of Snail1 increased 9.6-fold by 1 day after injury and 10-fold by 3 days after injury compared with the sham-operated group at 1 day after surgery ($P<0.05$) (Figure 2I).

Because epicardial cells are known to give rise to cardiomyocytes during development[20] and injury response,[22] we next examined Axin2-CreERT2–labeled cardiomyocytes at various time points. Although we observed that GFP expression marks rare cardiomyocytes in the subepicardial space of the ventricles, there was no significant difference in the number of GFP^+ cardiomyocytes at different time points in either injured or sham-operated mice, suggesting no significant contributions of GFP^+ epicardial cells to generate new cardiomyocytes. Taken together, our observations suggest that, following injury, Wnt-responsive epicardial cells proliferate and undergo EMT to give rise to cardiac fibroblasts that invaded the subepicardial space. Furthermore, at least a subset of GFP^+ cells were capable of becoming α-SMA^+ myofibroblasts. It is interesting to note that in the neonatal heart, GFP^+ epicardially derived cardiac fibroblasts were found

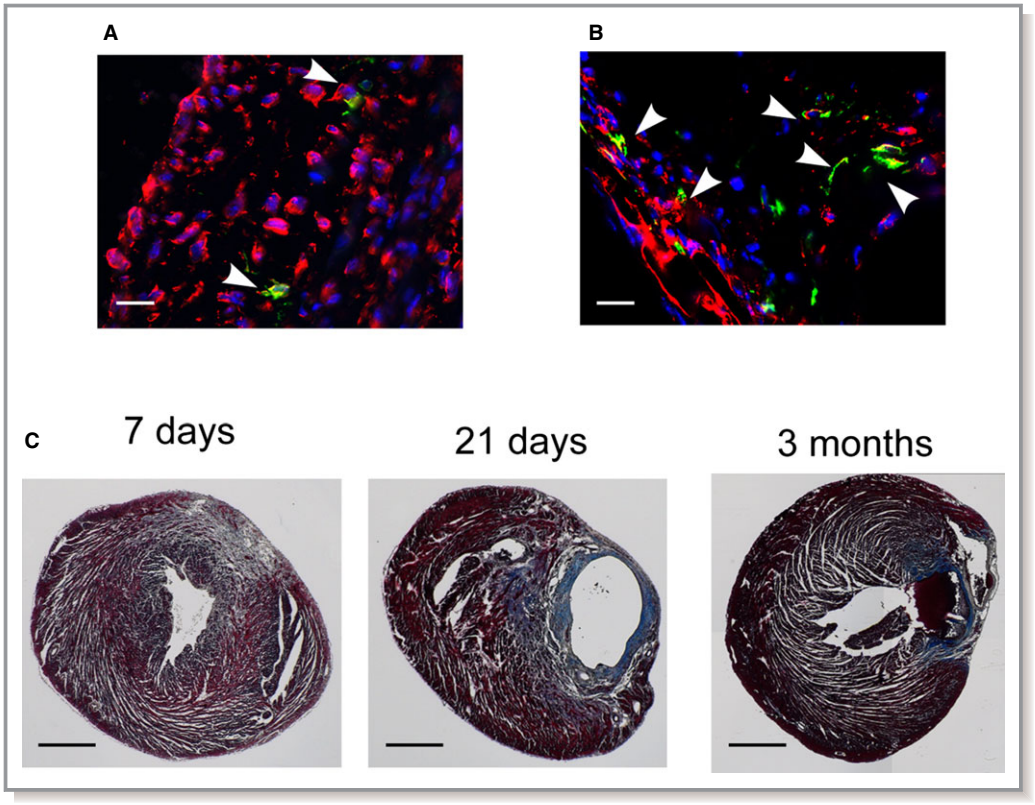

Figure 4. GFP and vimentin double-positive cardiac fibroblasts persisted for at least 8 weeks. Immunostaining against GFP (green) and vimentin (red) in Axin2-CreERT2;mTmG neonates that received tamoxifen injection either (A) before injury on P0 or (B) 9 days after injury on P10 and were traced for 8 weeks. Arrowheads indicate double-positive cells. Scale bar=20 μm. C, Trichrome staining of injured hearts at 7 days, 21 days, and 3 months after injury revealed extensive scarring that persisted to up to 3 months. Scale bar=0.5 mm.

within the subepicardial space following cryoinjury (Figure 2). In contrast, previous studies of the adult cardiac injury response have shown that epicardially derived cells underwent EMT but remained within the thickened epicardium.[1]

Cardiac Fibroblasts Become Wnt Responsive After Injury and Persist

Following adult cardiac injury, Wnt signaling is activated in various cell types.[2,10,24] We decided to examine whether Wnt signaling was induced following neonatal cryoinjury. Using Axin2-lacZ reporter mice, we examined Wnt signaling activation at various time points after cryoinjury (Figure 6A, 6B, and 6D). Using Masson's trichrome staining to identify the injured area, we observed an increase in lacZ signal at the edge of the infarcted area within the myocardium by 9 days after injury (Figure 6A, 6B, and 6D). Immunostaining against vimentin showed that some $lacZ^+$ cells colocalized with vimentin staining (54.6±6.9%) (Figure 6C, black arrowheads), whereas others did not (Figure 6C, white arrowheads). The lacZ staining within the myocardium was maintained for at least 21 days after injury.

To characterize the cells that become Wnt responsive after injury, we performed cryoinjury on Axin2-CreERT2;mTmG mice at P1, administered a dose of tamoxifen at 9 days after injury (when Axin2-lacZ expression was increased), and analyzed their hearts 48 hours thereafter. Similar to the Axin2-lacZ reporter mice, we observed more GFP^+ labeled cells in the myocardium of the border area adjacent to the infarct compared with the similar region in sham-operated controls (Figure 7A). Immunostaining of the hearts traced for 2 days showed that the majority of Wnt-responsive cells (95.6±3.8%) in the injury border zone coexpressed a fibroblast marker, vimentin (Figure 7B). The difference between the proportion of GFP^+ cells colocalizing with vimentin in Axin2-CreERT2;mTmG mice and the proportion of $lacZ^+$ cells costaining with vimentin may be related to a potential difference between the activation patterns of the 2 mouse strains. Unlike previous reports of adult injury,[2] we did not observe activation of Wnt signaling in endothelial cells.

We tracked these Wnt-responsive cardiac fibroblasts in vivo for various time periods. In the area adjacent to the infarct, at 21 days after tamoxifen administration, the percentage of GFP^+ cardiac fibroblasts was increased by a

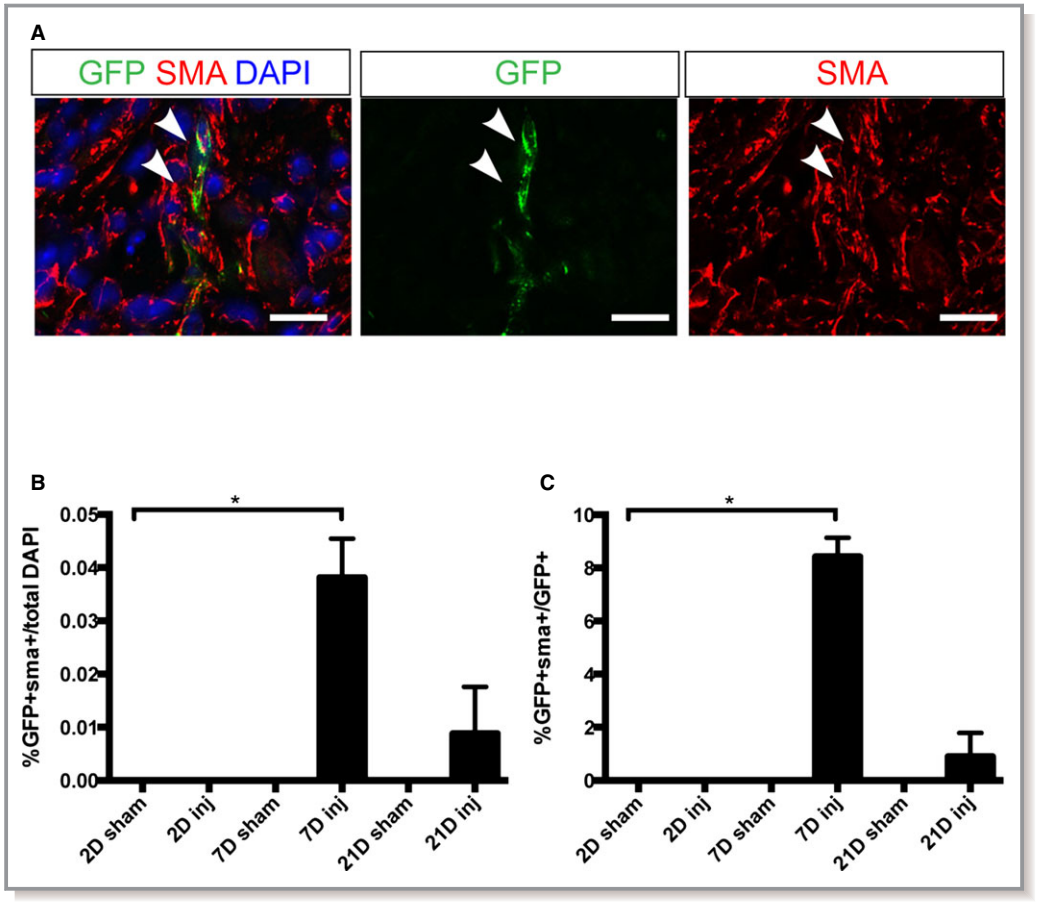

Figure 5. Some GFP$^+$ cells in Axin2-CreERT2;mTmG hearts expressed a myofibroblast marker, SMA. A, Immunostaining against GFP (green) and SMA (red) in Axin2-CreERT2;mTmG neonates that received tamoxifen before injury on P0 and were traced for 7 days. Arrowhead indicates double-positive cell. Scale bar=20 μm. B, Quantification of the percentage of GFP and SMA double-positive cells in the border area in injured hearts and the equivalent area in sham-operated hearts at 2, 7, and 21 days after labeling. C, Quantification of the percentage of GFP and SMA double-positive cells in total GFP$^+$ cells in the border area in injured hearts and the equivalent area in sham-operated hearts at 2, 7, and 21 days after labeling. Each group had at least 3 independent samples (n=3). Multiple fields (4–5) from an individual sample were imaged. Values are represented as mean±SEM. *denotes $P<0.05$. GFP indicates green fluorescent protein; SMA, α-smooth muscle actin.

factor of ≈7 compared with the short trace (48 hours; $P<0.05$) (Figure 7D). In addition, within the injured area at 21 days after labeling, there was a 9.5-fold increase in the percentage of GFP$^+$ cardiac fibroblasts compared with initial labeling ($P<0.05$) (Figure 7C). At 21 days after labeling, there was also a trend of an increase in the number of labeled cardiac fibroblasts in remote areas, suggesting more widespread activation of Wnt signaling in myocardium (Figure 7E). In sham-operated control hearts, there was no significant increase in the number of GFP$^+$ cells (Figure 7A, 7C, and 7D). In addition, we observed that the GFP$^+$ cardiac fibroblasts persisted in the infarct and the border areas for at least 56 days after tamoxifen administration (Figure 4B); however, unlike when Wnt-responsive cells were labeled before injury, we did not observe any GFP$^+$ cells that coexpressed α-SMA when labeling was done after injury. Our results show that cardiac fibroblasts in the neonatal heart become Wnt responsive and persist after cryoinjury.

Multiple Wnt Ligands Are Upregulated in Response to Cryoinjury

In addition to examining the characteristics of Wnt-responsive cells, we explored the identities of Wnt ligands that could be responsible for the increased Wnt signaling after cryoinjury. To this end, we surveyed the expression of all 19 Wnt ligands by in situ hybridization at 9 days after injury, when we observed an increase in the Axin2-lacZ reporter activity. Wnt ligand expression patterns fell into 5 patterns. The first category of Wnt ligands, including Wnt2b

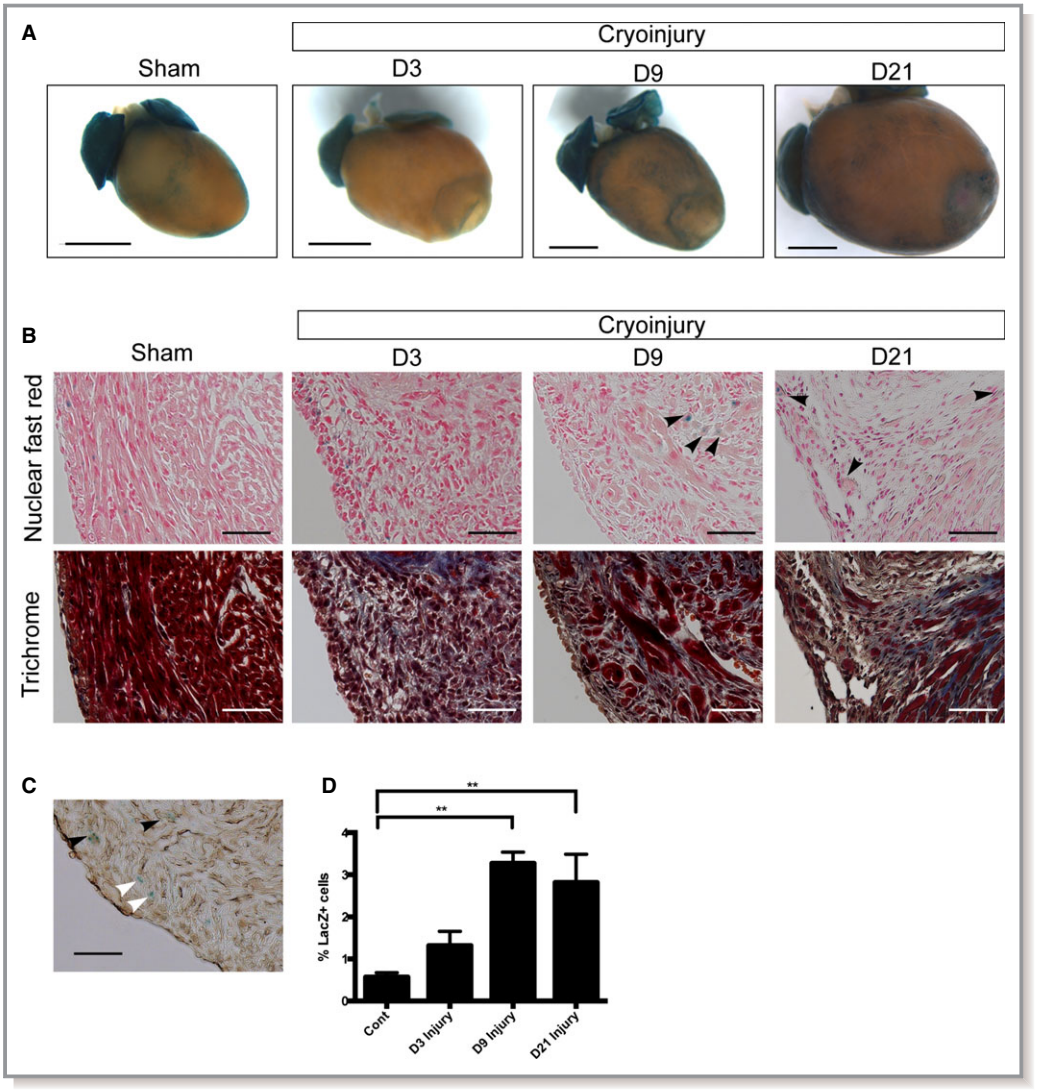

Figure 6. Activation of Wnt/β-catenin signaling in the injured neonatal heart. A, Whole-mount pictures of X-gal–stained hearts of Axin2-lacZ mice at 3, 9, and 21 days after injury. A whole-mount picture of the X-gal–stained sham-operated heart at 3 days after surgery is also shown. Scale bar=1 mm. B, X-gal and trichrome staining in serial sections showing the border area at 3, 9, and 21 days after injury and the equivalent area in the sham-operated heart. Arrowheads indicate lacZ-positive cells in the myocardium at 9 days after the injury. C, X-gal and vimentin staining (brown) showing that some lacZ-positive cells overlap (black arrowheads), whereas others do not (white arrowheads). D, Quantification of Axin2-lacZ positive cells in the border area at 3, 9, and 21 days after injury and the equivalent area in the sham-operated hearts at 3 days. Scale bar=100 μm. D indicates day. **denotes $P<0.01$.

and Wnt5a, showed very little to no expression in the sham-operated heart but a marked increase in the epicardium adjacent to the injured area (Figure 8A). The second category of ligands included Wnt9a, which showed no expression in the control but increased expression in the epicardium and the myocardium near the injury (Figure 8B). The third category of Wnt ligands had very little to no expression in the sham-operated heart and a slight increase in the myocardium close to the injury. The third category included Wnt3a, Wnt4, Wnt5b, Wnt6, Wnt8a, Wnt9b, and Wnt10b (Figure 8C). The fourth category of Wnt ligands showed very little to no expression in both the sham-operated heart and the injured heart (Figure 9). Wnt11 fell into a separate fifth category showing high expression levels in both sham-operated and injured hearts (Figure 9).

Identities of Wnt ligands upregulated following adult cardiac injury have been reported previously. Adult myocardial infarction resulted in increased expression of Wnt1, Wnt4, and Wnt7a[10] as well as Wnt2, Wnt10b, and Wnt11[2]; however, we found that the Wnt ligands that showed a more robust induction in the neonatal injury response (Wnt2b, Wnt5a, and Wnt9a) were different from the Wnt ligands with expression

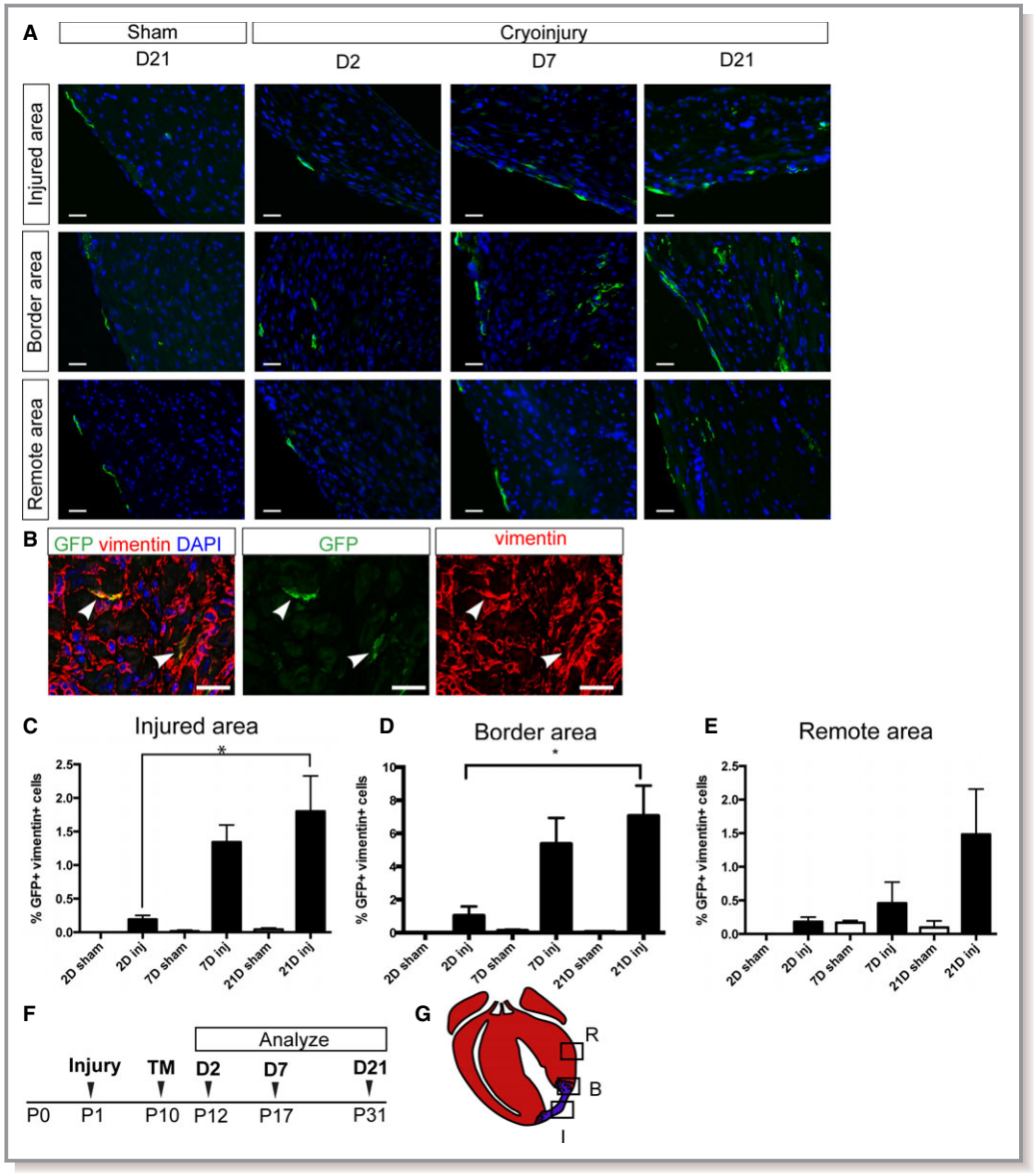

Figure 7. Cardiac fibroblasts become Wnt responsive and persist after injury. Axin2-CreERT2;mTmG neonates underwent cryoinjury or sham surgery on P1, were labeled at 9 days after injury on P10, and were sacrificed at various time points. A, Representative pictures of injured hearts showing injured areas, border areas, and remote areas at 2, 7, and 21 days after labeling. Corresponding areas from sham-treated heart at 21 days after labeling are also shown. Scale bar=20 μm. B, Immunostaining against GFP (green) and vimentin (red) in the injured heart at 2 days after labeling. Arrowheads indicate double-positive cells. Scale bar=20 μm. C through E, Quantification of the percentage of GFP and vimentin double-positive cells in (C) the injured area (D), the border area, and (E) the remote area in injured hearts and the equivalent areas in sham-operated hearts at 2, 7, and 21 days after labeling. Each group had at least 3 independent samples. Multiple fields (4–5) from an individual sample were imaged. Values are represented as mean±SEM. **P*<0.05. F, Schematic of the experimental time line. G, Diagram indicating the injured area, the border area, and the remote area. Red represents viable myocardium, and blue represents fibrotic tissue. B indicates border area; D, day; GFP, green fluorescent protein; I, injured area; Inj, injured; P, postnatal day; R, remote area; TM, tamoxifen.

that was increased in the adult cardiac injury response. Based on the current study, it is not clear whether distinct sets of Wnt ligands activate Wnt signaling differently in adult and neonatal cardiac fibroblasts.

Discussion

In the adult heart, excessive proliferation and subsequent deposition of extracellular matrix by cardiac fibroblasts lead to

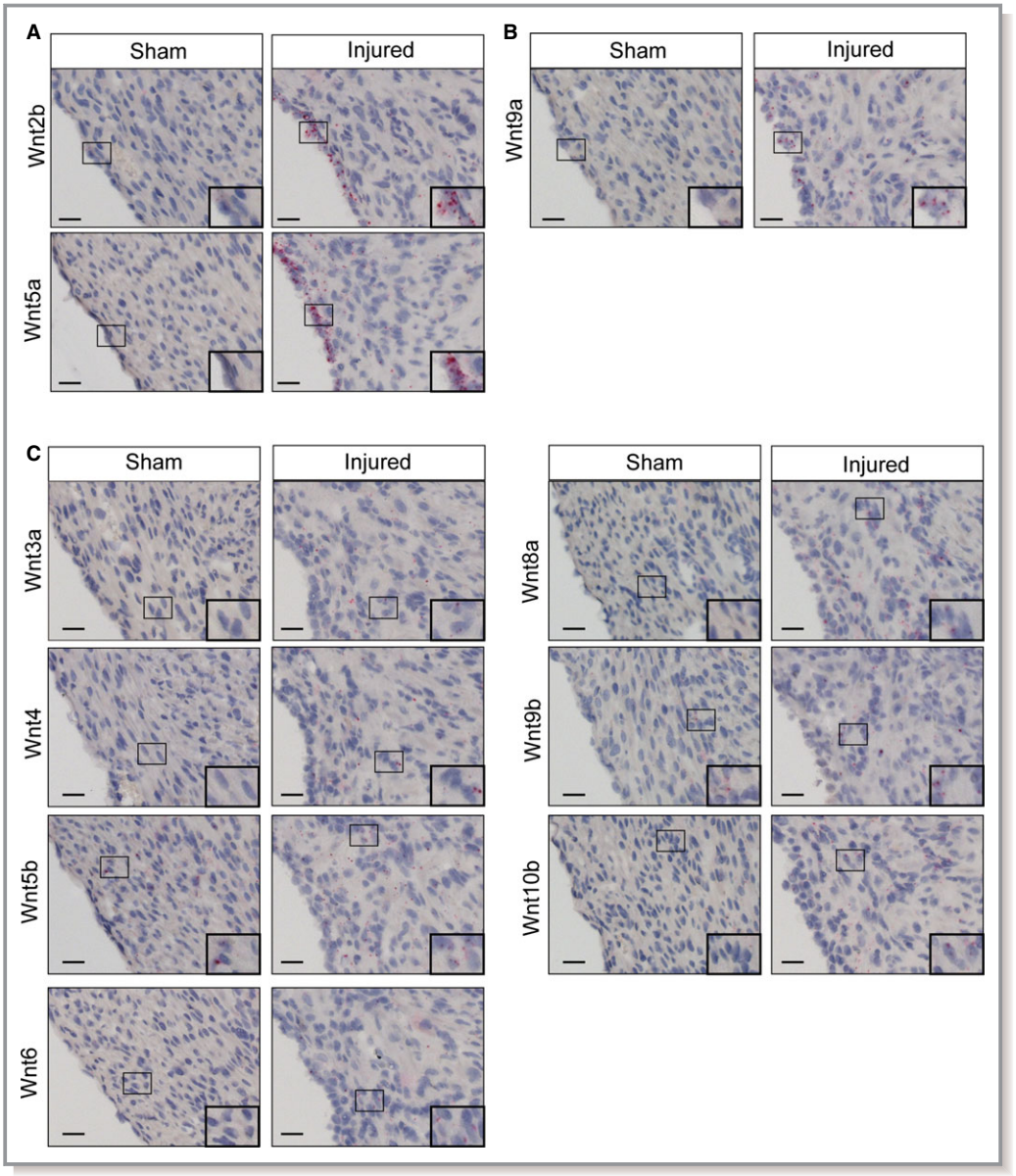

Figure 8. Wnt ligands are upregulated in the injured heart. RNA in situ hybridization of Wnt ligands in sham and cryoinjury hearts at 9 days after surgery. A, Wnt2b and Wnt5a are upregulated in epicardium of the injured heart. B, Wnt9a is upregulated in epicardium and myocardium of the injured heart. C, Wnt 3a, Wnt4, Wnt5b, Wnt6, Wnt8a, Wnt9b, and Wnt10b are upregulated in myocardium of the injured heart. Scale bar=20 μm.

scar formation that eventually causes heart failure; therefore, it is of great interest to understand how fibrosis is regulated. Although scar formation in the adult heart has been studied extensively, it is not known how the development of fibrosis is regulated in the neonatal heart. Our results show that Wnt-responsive epicardial cells and cardiac fibroblasts contribute to scar formation in the neonatal heart.

Using Axin2, a well-established Wnt/β-catenin signaling target gene, as a marker for Wnt-activated cells, we found that epicardial cells in the uninjured neonatal heart were Wnt responsive (Figure 1A through 1D). Although it has been known that Wnt/β-catenin signaling in the embryonic proepicardium is critical for heart development,[21,25] active Wnt signaling in the epicardium of the uninjured postnatal heart had not been characterized previously. In the uninjured adult heart, Wnt/β-catenin signaling has been observed in blood vessels and the valves using TOPGAL reporter mice.[2] Our analysis of Axin2-lacZ heart also revealed active Wnt/β-catenin signaling in the valves and atrial cardiomyocytes (Figure 1C and 1D).

Using Axin2-CreERT2;mTmG mice, we showed that the Wnt-responsive epicardial cells of the neonatal heart prolif-

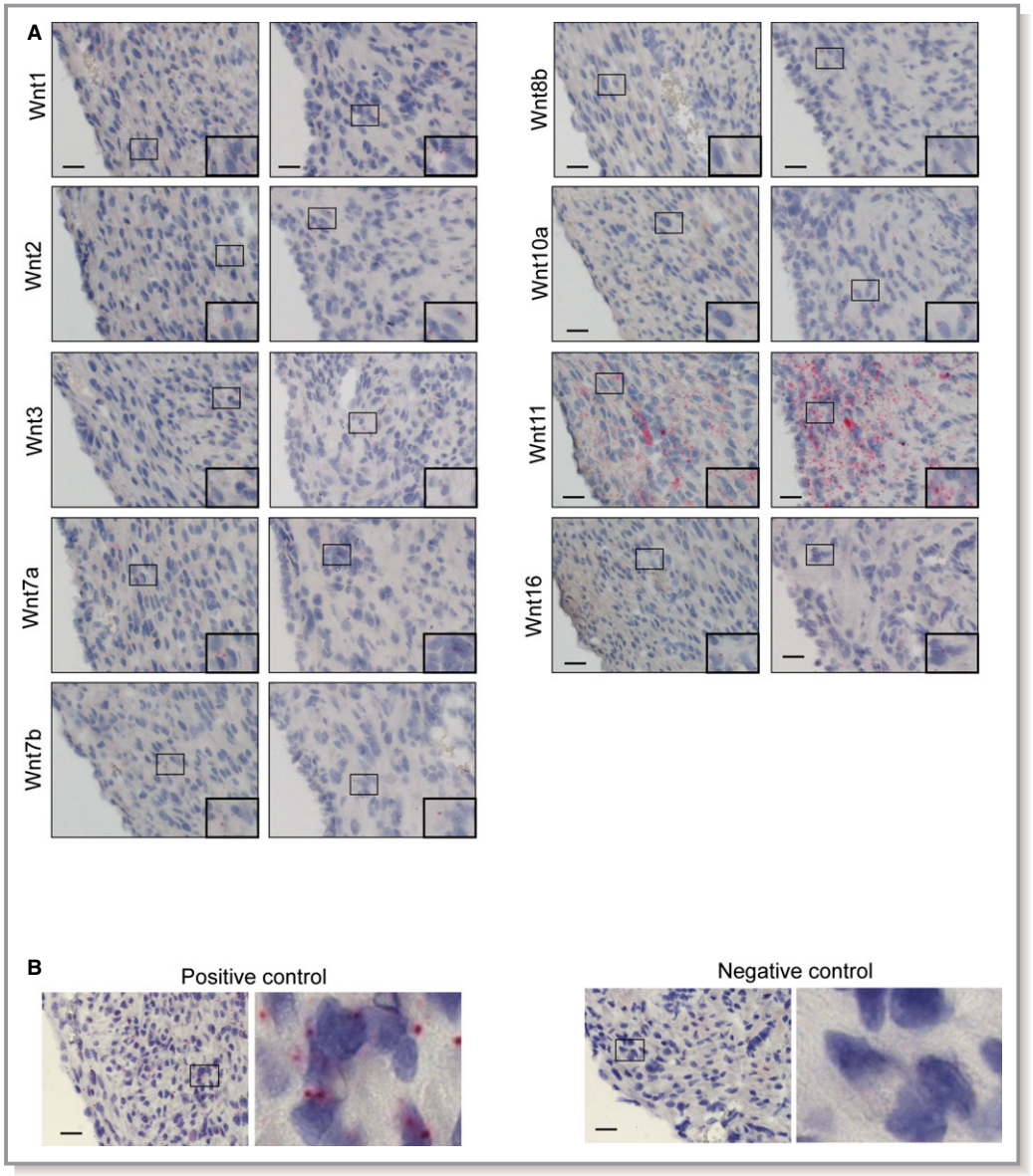

Figure 9. Wnt ligands with expression that does not change after injury. A, Wnt1, Wnt2, Wnt3, Wnt7a, Wnt7b, Wnt8b, Wnt10a, Wnt11, and Wnt16 expression are not affected in the injured heart. B, A positive control (Pol2a, a housekeeping gene) and a negative control (DapB, a bacterial gene) for RNA in situ are shown. Scale bar=20 μm.

erated in response to cryoinjury and gave rise to cardiac fibroblasts and activated myofibroblasts via EMT (Figures 2 and 5). Because we did observe very rare Wnt-responsive cardiac fibroblasts prior to injury, we cannot formally rule out the possibility that Axin2-CreERT2–labeled fibroblasts originated from preexisting Wnt-responsive cardiac fibroblasts; however, the contribution of these Wnt-responsive cardiac fibroblasts is likely to be minor, given that they were very rare, accounting for <0.05% of cells. In contrast, the ability of epicardial cells to give rise to fibroblasts in the embryonic heart[26] and in response to adult cardiac injury[10,27] has been demonstrated previously. Taken together with previous reports, our observations support the idea that Wnt-responsive epicardial cells participate in fibrosis in the neonatal heart. Although epicardial cells are also known to give rise to other cell types such as cardiomyocytes after injury,[22] we did not detect such contribution from Wnt-responsive epicardial cells.

We also found that neonatal cardiac fibroblasts in the myocardium became Wnt-responsive following cryoinjury (Figure 6). Similar activation of Wnt signaling in cardiac fibroblasts has been observed in adult heart after ischemic injury.[2,10] Lineage-tracing experiments using Axin2-CreERT2; mTmG mice revealed that the myocardial cardiac fibroblasts

that became Wnt responsive after injury persisted in the neonatal heart (Figures 6 and 7). Interestingly, these Wnt-responsive cells did not colocalize with the α-SMA marker. This observation suggests the possibility that cardiac fibroblasts that become Wnt responsive in response to injury are a different population of cardiac fibroblasts that are derived from Wnt-responsive epicardial cells. A future investigation characterizing these different cardiac fibroblast populations may yield interesting insights into the mechanisms of cardiac injury response.

Wnt signaling has been associated with both EMT and activation of resident cardiac fibroblasts in the injured adult heart.[2,10,11] Our RNA in situ screen of all 19 Wnt ligands revealed an interesting difference in the identities of Wnt ligands that are upregulated in the neonatal heart following injury. Multiple Wnt ligands including Wnt3a, Wnt4, Wnt5b, Wnt6, Wnt8a, Wnt9a, Wnt9b, and Wnt10b showed elevated expression in the myocardium near the injury site (Figure 8B and 8C). In contrast, a previous study identified upregulation of Wnt1, Wnt4, and Wnt7a,[10] and another study reported upregulation of Wnt2, Wnt10b, and Wnt11[2] based on quantitative polymerase chain reaction analysis of the ischemic adult heart. Of particular interest is the identity of Wnt ligands that are highly upregulated in the epicardium. In the neonatal epicardium, Wnt2b and Wnt5a were upregulated following cryoinjury (Figure 8A), whereas in the adult epicardium, upregulation of Wnt1 has been reported.[10] Interestingly, Wnt5a function has been implicated in embryonic EMT.[28] Our observation that neonatal heart injury results in Wnt5a upregulation may suggest that the neonatal heart retains embryonic characteristics and that there are multiple ways in which Wnt signaling promotes EMT depending on the developmental stage and/or the nature of injury. It is interesting to note that Wnt signaling has been implicated in EMT in various other contexts such as primitive streak formation in developing embryos[29,30] and cancer progression.[31,32] In interpreting the current result, it is important to keep in mind that quantitative polymerase chain reaction analysis of whole heart tissue may not detect more spatially restricted upregulation of certain ligands. Furthermore, to fully appreciate the complexity of Wnt signaling, it is crucial to investigate cell-specific expression of different Wnt receptors and coreceptors. Consequently, future investigation of Wnt signaling in the cardiac injury response should also assess potential differences in Wnt receptor expression patterns between adult and neonatal hearts.

In this study, we unexpectedly observed extensive and persistent scar formation in the neonatal heart following cryoinjury using the method described previously[5] (Figure 4). Previous reports of cryoinjury in the neonatal heart showed minimal scarring and significant scar regression.[5,6] Such robust regenerative capacity of the neonatal heart has also been demonstrated following other types of injury, including apical resection[3] and left anterior descending artery ligation.[4] The discrepancy between our observations and previous reports may be caused by technical variations that resulted in different severity of the initial injury. Other possible factors are differences in mouse strains, which have been shown to influence the degree of scar formation in the adult injury response.[33] Although it is not possible to determine the cause of the different outcomes, our results suggest that severe cryoinjury can overwhelm the regenerative capacity of the neonatal heart. It is interesting to note that our observation is consistent with a report that cryoinjury in zebrafish heart resulted in more extensive scar formation and delayed scar regression compared with apical resection.[34] It is possible that the nature of cryoinjury itself renders regeneration more challenging, even to the neonatal heart. Compared with apical resection in which the apex of the heart is excised, cryoinjury may cause more severe inflammation because more dead cells need to be cleared. In addition, careful comparison of the fibrotic responses to cryoinjury and left anterior descending artery ligation may reveal a difference in fibrotic tissue formation, leading one to be cleared and the other to persist as scar.

In summary, cryoinjury in the neonatal heart leads to activation of Wnt signaling in the epicardium as well as the myocardium. Furthermore, we identified different Wnt ligands that may play a role in regulation of scar formation in the neonatal heart compared with the adult heart. Our results highlight the need to pay attention to the subtle differences in components of Wnt signaling such as the identities of Wnt ligands during the cardiac injury response. Although activation of Wnt signaling may be limited to a small number of cells within the injured neonatal heart, multiple lines of observation based on the specific activation patterns of Axin2-lacZ, Axin2-CreERT2, and Wnt ligand expression suggest a biological function for Wnt signaling. A future investigation comparing the differences in the mechanisms of Wnt signaling in cryoinjury and other cardiac injury models in the neonatal heart may lead to valuable insight into what limits cardiac regeneration.

Acknowledgments

We would like to thank Kate Brown and Catriona Logan for critical reading of the manuscript and discussion. We would like to thank Neil Willits at the statistical consulting service at the Department of Statistics at UC Davis for his statistical help.

Sources of Funding

Mizutani was supported by Stanford Graduate Fellowship. Nusse is an investigator of the Howard Hughes Medical Institute.

Disclosures

None.

References

1. Zhou B, Honor LB, He H, Ma Q, Oh J-H, Butterfield C, Lin R-Z, Melero-Martin JM, Dolmatova E, Duffy HS, Gise AV, Zhou P, Hu YW, Wang G, Zhang B, Wang L, Hall JL, Moses MA, McGowan FX, Pu WT. Adult mouse epicardium modulates myocardial injury by secreting paracrine factors. *J Clin Invest*. 2011;121:1894–1904.
2. Aisagbonhi O, Rai M, Ryzhov S, Atria N, Feoktistov I, Hatzopoulos AK. Experimental myocardial infarction triggers canonical Wnt signaling and endothelial-to-mesenchymal transition. *Dis Model Mech*. 2011;4:469–483.
3. Porrello ER, Mahmoud AI, Simpson E, Hill JA, Richardson JA, Olson EN, Sadek HA. Transient regenerative potential of the neonatal mouse heart. *Science*. 2011;331:1078–1080.
4. Porrello ER, Mahmoud AI, Simpson E, Johnson BA, Grinsfelder D, Canseco D, Mammen PP, Rothermel BA, Olson EN, Sadek HA. Regulation of neonatal and adult mammalian heart regeneration by the miR-15 family. *Proc Natl Acad Sci USA*. 2013;110:187–192.
5. Strungs EG, Ongstad EL, O'Quinn MP, Palatinus JA, Jourdan LJ, Gourdie RG. Cryoinjury models of the adult and neonatal mouse heart for studies of scarring and regeneration. In: Gourdie GG, Tereance MA, eds. *Methods in Molecular Biology*. Vol. 1037. Totowa, NJ: Humana Press; 2013:343–353.
6. Jesty SA, Steffey MA, Lee FK, Breitbach M, Hesse M, Reining S, Lee JC, Doran RM, Nikitin AY, Fleischmann BK, Kotlikoff MI. c-kit+ precursors support postinfarction myogenesis in the neonatal, but not adult, heart. *Proc Natl Acad Sci USA*. 2012;109:13380–13385.
7. Porrello ER, Johnson BA, Aurora AB, Simpson E, Nam YJ, Matkovich SJ, Dorn GW, van Rooij E, Olson EN. MiR-15 family regulates postnatal mitotic arrest of cardiomyocytes. *Circ Res*. 2011;109:670–679.
8. Xin M, Kim Y, Sutherland LB, Murakami M, Qi X, McAnally J, Porrello ER, Mahmoud AI, Tan W, Shelton JM, Richardson JA, Sadek HA, Bassel-Duby R, Olson EN. Hippo pathway effector Yap promotes cardiac regeneration. *Proc Natl Acad Sci USA*. 2013;110:13839–13844.
9. Deb A. Cell-cell interaction in the heart via Wnt/β-catenin pathway after cardiac injury. *Cardiovasc Res*. 2014;102:214–223.
10. Duan J, Gherghe C, Liu D, Hamlett E, Srikantha L, Rodgers L, Regan JN, Rojas M, Willis M, Leask A, Majesky M, Deb A. Wnt1/βcatenin injury response activates the epicardium and cardiac fibroblasts to promote cardiac repair. *EMBO J*. 2012;31:429–442.
11. Laeremans H, Hackeng TM, van Zandvoort MAMJ, Thijssen VLJL, Janssen BJA, Ottenheijm HCJ, Smits JFM, Blankesteijn WM. Blocking of frizzled signaling with a homologous peptide fragment of Wnt3a/Wnt5a reduces infarct expansion and prevents the development of heart failure after myocardial infarction. *Circulation*. 2011;124:1626–1635.
12. Barandon L, Couffinhal T, Ezan J, Dufourcq P, Costet P, Alzieu P, Leroux L, Moreau C, Dare D, Duplàa C. Reduction of infarct size and prevention of cardiac rupture in transgenic mice overexpressing FrzA. *Circulation*. 2003;108:2282–2289.
13. He W, Zhang L, Ni A, Zhang Z, Mirotsou M, Mao L, Pratt RE, Dzau VJ. Exogenously administered secreted frizzled related protein 2 (Sfrp2) reduces fibrosis and improves cardiac function in a rat model of myocardial infarction. *Proc Natl Acad Sci USA*. 2010;107:21110–21115.
14. Hahn J-Y, Cho H-J, Bae J-W, Yuk H-S, Kim K-I, Park K-W, Koo B-K, Chae I-H, Shin C-S, Oh B-H, Choi Y-S, Park Y-B, Kim H-S. Beta-catenin overexpression reduces myocardial infarct size through differential effects on cardiomyocytes and cardiac fibroblasts. *J Biol Chem*. 2006;281:30979–30989.
15. Lustig B, Jerchow B, Sachs M, Weiler S, Pietsch T, Karsten U, van de Wetering M, Clevers H, Schlag PM, Birchmeier W, Behrens J. Negative feedback loop of Wnt signaling through upregulation of conductin/axin2 in colorectal and liver tumors. *Mol Cell Biol*. 2002;22:1184–1193.
16. van Amerongen R, Bowman AN, Nusse R. Developmental stage and time dictate the fate of Wnt/β-catenin-responsive stem cells in the mammary gland. *Cell Stem Cell*. 2012;11:387–400.
17. Muzumdar MD, Tasic B, Miyamichi K, Li L, Luo L. A global double-fluorescent Cre reporter mouse. *Genesis*. 2007;45:593–605.
18. Wang F, Flanagan J, Su N, Wang L-C, Bui S, Nielson A, Wu X, Vo H-T, Ma X-J, Luo Y. RNAscope: a novel in situ RNA analysis platform for formalin-fixed, paraffin-embedded tissues. *J Mol Diagn*. 2012;14:22–29.
19. Jho E-H, Zhang T, Domon C, Joo C-K, Freund J-N, Costantini F. Wnt/beta-catenin/Tcf signaling induces the transcription of Axin2, a negative regulator of the signaling pathway. *Mol Cell Biol*. 2002;22:1172–1183.
20. Zhou B, Ma Q, Rajagopal S, Wu SM, Domian I, Rivera-Feliciano J, Jiang D, von Gise A, Ikeda S, Chien KR, Pu WT. Epicardial progenitors contribute to the cardiomyocyte lineage in the developing heart. *Nature*. 2008;454:109–113.
21. Zamora M, Männer J, Ruiz-Lozano P. Epicardium-derived progenitor cells require beta-catenin for coronary artery formation. *Proc Natl Acad Sci USA*. 2007;104:18109–18114.
22. Smart N, Bollini S, Dubé KN, Vieira JM, Zhou B, Davidson S, Yellon D, Riegler J, Price AN, Lythgoe MF, Pu WT, Riley PR. De novo cardiomyocytes from within the activated adult heart after injury. *Nature*. 2011;474:640–644.
23. Cai C-L, Martin JC, Sun Y, Cui L, Wang L, Ouyang K, Yang L, Bu L, Liang X, Zhang X, Stallcup WB, Denton CP, McCulloch A, Chen J, Evans SM. A myocardial lineage derives from Tbx18 epicardial cells. *Nature*. 2008;454:104–108.
24. Oerlemans MIFJ, Goumans M-J, van Middelaar B, Clevers H, Doevendans PA, Sluijter JPG. Active Wnt signaling in response to cardiac injury. *Basic Res Cardiol*. 2010;105:631–641.
25. Merki E, Zamora M, Raya A, Kawakami Y, Wang J, Zhang X, Burch J, Kubalak SW, Kaliman P, Izpisúa-Belmonte JC, Chien KR, Ruiz-Lozano P. Epicardial retinoid X receptor alpha is required for myocardial growth and coronary artery formation. *Proc Natl Acad Sci USA*. 2005;102:18455–18460.
26. Wessels A, van den Hoff MJB, Adamo RF, Phelps AL, Lockhart MM, Sauls K, Briggs LE, Norris RA, van Wijk B, Pérez-Pomares JM, Dettman RW, Burch JBE. Epicardially derived fibroblasts preferentially contribute to the parietal leaflets of the atrioventricular valves in the murine heart. *Dev Biol*. 2012;366:111–124.
27. Ali SR, Ranjbarvaziri S, Talkhabi M, Zhao P, Subat A, Hojjat A, Kamran P, Muller AMS, Volz KS, Tang Z, Red-Horse K, Ardehali R. Developmental heterogeneity of cardiac fibroblasts does not predict pathological proliferation and activation. *Circ Res*. 2014;115:625–635.
28. von Gise A, Zhou B, Honor LB, Ma Q, Petryk A, Pu WT. WT1 regulates epicardial epithelial to mesenchymal transition through β-catenin and retinoic acid signaling pathways. *Dev Biol*. 2011;356:421–431.
29. ten Berge D, Koole W, Fuerer C, Fish M, Eroglu E, Nusse R. Wnt signaling mediates self-organization and axis formation in embryoid bodies. *Cell Stem Cell*. 2008;3:508–518.
30. Liu P, Wakamiya M, Shea MJ, Albrecht U, Behringer RR, Bradley A. Requirement for Wnt3 in vertebrate axis formation. *Nat Genet*. 1999;22:361–365.
31. Bo H, Zhang S, Gao L, Chen Y, Zhang J, Chang X, Zhu M. Upregulation of Wnt5a promotes epithelial-to-mesenchymal transition and metastasis of pancreatic cancer cells. *BMC Cancer*. 2013;13:496.
32. Brabletz T, Jung A, Reu S, Porzner M, Hlubek F, Kunz-Schughart LA, Knuechel R, Kirchner T. Variable beta-catenin expression in colorectal cancers indicates tumor progression driven by the tumor environment. *Proc Natl Acad Sci USA*. 2001;98:10356–10361.
33. van den Borne SWM, van de Schans VAM, Strzelecka AE, Vervoort-Peters HTM, Lijnen PM, Cleutjens JPM, Smits JFM, Daemen MJAP, Janssen BJA, Blankesteijn WM. Mouse strain determines the outcome of wound healing after myocardial infarction. *Cardiovasc Res*. 2009;84:273–282.
34. González-Rosa JM, Martín V, Peralta M, Torres M, Mercader N. Extensive scar formation and regression during heart regeneration after cryoinjury in zebrafish. *Development*. 2011;138:1663–1674.